High gain observer for speed-sensorless motor drives: algorithm and experiments

Wang, Y.; Zhou, L.; Bortoff, S.A.; Satake, A.; Furutani, S.

TR2016-089 July 2016

Abstract

This paper considers the rotor speed and flux estimation for induction motors, which is one of the key problems in speed-sensorless motor drives. Existing approaches, e.g. adaptive, Kalman filter-based, and sliding mode observer, have limitations such as unnecessarily assuming the rotor speed as a constant parameter, failure to ensure convergence of estimation error dynamics, or conservative design. This paper proposes a nontriangular observable form-based estimation algorithm. This paper presents realizable observers to avoid transforming the induction motor model into the form. Advantages of the new estimation algorithm include guaranteed stability of estimation error dynamics, constructive observer design, ease of tuning, and improved speed estimation performance. Finally, experiments are conducted to demonstrate the effectiveness of the proposed estimation algorithm.

IEEE International Conference on Advanced Intelligent Mechatronics

High gain observer for speed-sensorless motor drives: algorithm and experiments

Yebin Wang, Lei Zhou, Scott A. Bortoff, Akira Satake, and Shinichi Furutani

***Abstract*—This paper considers the rotor speed and flux estimation for induction motors, which is one of the key problems in speed-sensorless motor drives. Existing approaches, e.g. adaptive, Kalman filter-based, and sliding mode observer, have limitations such as unnecessarily assuming the rotor speed as a constant parameter, failure to ensure convergence of estimation error dynamics, or conservative design. This paper proposes a non-triangular observable form-based estimation algorithm. This paper presents realizable observers to avoid transforming the induction motor model into the form. Advantages of the new estimation algorithm include guaranteed stability of estimation error dynamics, constructive observer design, ease of tuning, and improved speed estimation performance. Finally, experiments are conducted to demonstrate the effectiveness of the proposed estimation algorithm.**

I. Introduction

Speed-sensorless motor drives have attracted much attention not only because removing the rotor shaft encoder reduces the system cost and improves reliability, but also because the resultant control and estimation design is challenging [1]–[3]. The rotor speed estimation from current sensors, instead of the encoder, is commonly unsatisfactory. Speed-sensorless motor drives suffer significant performance degradation, and are limited to fields requiring low or medium performance. Significant efforts have been devoted to lifting this bottleneck.

Adaptation idea, where the rotor speed is treated as an unknown parameter to avoid dealing with nonlinear dynamics, was initially exploited and remains appealing due to simplicity [4]–[8]. Adaptation-based estimation suffers slow transience. This motivates nonlinear estimator designs, e.g. , high gain [3], [9], sliding mode [10], [11], and extended/unscented Kalman filter [12]–[14], etc. Nonlinear observer design typically entails the system in normal forms. For instance, high gain and sliding mode observer designs assume an observable form in triangular structures [15], [16]. With stator current measurements, the induction motor model does not admit the observable form.

This paper develops and verifies a new algorithm for speed-sensorless motor drives. Main contributions are three-fold: first, with uniformly observable assumption, we show that the induction motor model admits a non-triangular observable form by a change of state coordinates, and perform high gain observer design based on work [17]; second, we propose several implementable observers without the closed-form expression of the inverse state transformation; finally, we validate the proposed algorithm by experiments.

The rest of this paper is organized as follows. Problem formulation is provided in Section II. Section III presents speed-sensorless estimation algorithms. Experimental results in Section IV verify that the proposed algorithm is meaningful and effective in practice. This paper is concluded by Section V.

Y. Wang and S. A. Bortoff are with Mitsubishi Electric Research Laboratories, Cambridge, MA 02139, USA (email: yebinwang@ieee.org, bortoff@merl.com).

L. Zhou is with the Department of Mechanical Engineering, Massachusetts Institute of Technology, Cambridge, MA 02139, USA (email: leizhou@mit.edu).

A. Satake and S. Furutani are with the Advanced Technology R&D Center, Mitsubishi Electric Corporation, 8-1-1, Tsukaguchi-honmachi, Amagasaki City, 661–8661, Japan (email: Satake.Akira@dy.MitsubishiElectric.co.jp, Furutani.Shinichi@dw.MitsubishiElectric.co.jp).

II. Problem Statement

The induction motor model, in a frame rotating at an angular speed ω_1, is given by

$$\begin{aligned}
\dot{i}_{ds} &= -\gamma i_{ds} + \omega_1 i_{qs} + \beta(\alpha\Phi_{dr} + p\omega\Phi_{qr}) + \frac{u_{ds}}{\sigma}\\
\dot{i}_{qs} &= -\omega_1 i_{ds} - \gamma i_{qs} + \beta(\alpha\Phi_{qr} - p\omega\Phi_{dr}) + \frac{u_{qs}}{\sigma}\\
\dot{\Phi}_{dr} &= -\alpha\Phi_{dr} + (\omega_1 - p\omega)\Phi_{qr} + \alpha L_m i_{ds}\\
\dot{\Phi}_{qr} &= -\alpha\Phi_{qr} - (\omega_1 - p\omega)\Phi_{dr} + \alpha L_m i_{qs}\\
\dot{\omega} &= \mu(\Phi_{dr} i_{qs} - \Phi_{dr} i_{qs}) - \frac{T_l}{J}\\
y &= \begin{pmatrix} i_{ds} & i_{qs}\end{pmatrix}^\top,
\end{aligned} \tag{1}$$

where notation is defined in Table I. The frame with $\omega_1 = 0$ is typically called the stator or stationary frame. Throughout this paper, we take $\omega_1 = 0$. Readers are referred to [18], [19] for details on induction motor modeling.

Letting ζ be a dummy variable, for the rest of this paper, we denote $\hat{\zeta}$ as the estimate of the variable, ζ^* as the reference, $\tilde{\zeta} = \zeta - \hat{\zeta}$ as the estimation error, and $e_\zeta = \zeta^* - \zeta$ or $e_\zeta = \zeta^* - \hat{\zeta}$ as the tracking error. Given a C^∞ vector field $f : \mathbb{R}^n \to \mathbb{R}^n$, and a C^∞ function $h : \mathbb{R}^n \to \mathbb{R}$, the function $L_f h(\zeta) = \frac{\partial h(\zeta)}{\partial \zeta} f$ is the *Lie derivative* of $h(\zeta)$ along f. Repeated Lie derivatives are defined as $L_f^k h(\zeta) = L_f(L_f^{k-1} h(\zeta))$, $k \geq 1$ with $L_f^0 h(\zeta) = h(\zeta)$.

This paper deals with the state estimation of the following speed-sensorless control problem.

Problem 1: Given the induction motor model (1), the rotor speed reference trajectory ω^*, and the rotor flux amplitude reference ϕ^*, determine controls u_{sa} and u_{sb} so that the rotor speed ω and the rotor flux amplitude $\sqrt{\Phi_{dr}^2 + \Phi_{qr}^2}$ are regulated to their references, respectively.

Work [20] shows the existence of operation regimes that the model (1) is neither observable nor detectable. Lack of local (uniform) observability poses fundamental limitation to

TABLE I
NOTATIONS

Notation	Description
i_{ds}, i_{qs}	stator currents in d- and q-axis
Φ_{dr}, Φ_{qr}	rotor fluxes in d- and q-axis
ω	rotor angular speed
u_{ds}, u_{qs}	stator voltages in d- and q-axis
ω_1	angular speed of a rotating frame
Φ^*_{dr}	rotor flux amplitude reference
ω^*	rotor angular speed reference
i^*_{ds}, i^*_{qs}	references of stator currents in d- and q-axis
T_l	load torque
J	inertia
L_s, L_m, L_r	stator, mutual, and rotor inductances
R_s, R_r	stator and rotor resistances
σ	$\frac{L_s L_r - L_m^2}{L_r}$
α	R_r/L_r
β	$L_m/(\sigma L_r)$
γ	$R_s/\sigma + \alpha\beta L_m$
μ	$3L_m/(2JL_r)$

Problem 1. For simplicity, this paper assumes that operation conditions suffice the uniform observability, and concentrates on state estimator design.

III. Speed-sensorless Estimator Design

Consider a locally uniformly observable multi-input and multi-output (MIMO) system represented by

$$\begin{aligned}\dot{\zeta} &= f(\zeta) + g(\zeta)u \\ y &= h(\zeta),\end{aligned} \tag{2}$$

where the state $\zeta \in \mathbb{R}^n$, the control input $u \in \mathbb{R}^m$, the output $y \in \mathbb{R}^p$, $f, g : \mathbb{R}^n \to \mathbb{R}^n$ are C^∞ vector fields, and $h : \mathbb{R}^n \to \mathbb{R}^p$ is a vector of C^∞ functions. System (2) is not in structures which allow convergence-guaranteed nonlinear observer designs, e.g. exact error linearization [21]–[24], block triangular-based decentralized observer [25]–[27], high gain observer [15], and sliding mode observer [10], [11], [28].

A. A Non-triangular Observable Form

Work in [17] assumes that system (2) is transformable to the following non-triangular observable form by a change of state coordinates $x = \phi(\zeta)$

$$\begin{aligned}\dot{x} &= Ax + \varphi(x, u) \\ y &= Cx,\end{aligned} \tag{3}$$

where the state $x \in \mathbb{R}^n$, and for $1 \le k \le p$, $x = \begin{bmatrix}(x^1)^\top & \dots & (x^p)^\top\end{bmatrix}^\top, x^k = \begin{bmatrix}x^k_1 & \dots & x^k_{\lambda_k}\end{bmatrix}^\top \in \mathbb{R}^{\lambda_k}$, and

$$\begin{aligned}A &= \text{diag}\{A_1, \cdots, A_p\},\ A_k = \begin{bmatrix}0 & I_{\lambda_k - 1} \\ 0 & 0\end{bmatrix} \in \mathbb{R}^{\lambda_k \times \lambda_k} \\ C &= \text{diag}\{C_1, \dots, C_p\},\ C_k = \begin{bmatrix}1 & 0\end{bmatrix} \in \mathbb{R}^{\lambda_k}.\end{aligned}$$

Literally, x^k denotes the state of the kth subsystem associated with the kth output y_k, and $\lambda_k, 1 \le k \le p$ are the dimensions of all subsystems. We call λ_k for $1 \le k \le p$ as subsystem indices and have $\sum_{k=1}^p \lambda_k = n$. Note that the vector field $\varphi(x, u)$ is described as $\varphi = \begin{bmatrix}(\varphi^1)^\top & \dots & (\varphi^p)^\top\end{bmatrix}^\top, \varphi^k = \begin{bmatrix}\varphi^k_1 & \dots & \varphi^k_{\lambda_k}\end{bmatrix}^\top \in \mathbb{R}^{\lambda_k},\ 1 \le k \le p$. Specifically, φ^k_i has the following structure: for $1 \le i \le \lambda_k - 1$,

$$\varphi^k_i = \varphi^k_i(x^1, \cdots, x^{k-1}, x^k_1, \cdots, x^k_i, x^{k+1}_1, \cdots, x^p_1, u) \tag{4}$$

and for $i = \lambda_k$, $\varphi^k_i = \varphi^k_{\lambda_k}(x^1, \cdots, x^p, u)$.

Remark 3.1: The non-triangular observable form (3) is a special case of the form defined in [17, Eqn. (1)] by taking $p_k = 1$. In fact, taking $p_k = 1$ for $1 \le k \le q$ in [17, Eqn. (1)] gives $q = p$ and $\lambda_k = n_k$.

Remark 3.2: It is challenging to verify that system (2) is transformable to (3). It is more difficult to solve $x = \phi(\zeta)$ and its inverse $\zeta = \phi^{-1}(x)$. Verifying the transformability and solving the state transformation comprise another portfolio of research topics which are not covered here.

B. Design Procedure for Case 1: $\zeta = \phi^{-1}(x)$ Solvable

Given system in the non-triangular observable form (3), work [17] performs observer design to estimate x. Afterwards, estimates of ζ, denoted by $\hat{\zeta}$, is reconstructed from $\hat{x}$.

1) Observer design in x-coordinates: The observer for the kth subsystem is

$$\begin{aligned}\dot{\hat{x}}^k &= A_k \hat{x}^k + \hat{\varphi}^k + \theta^{\delta_k} \Delta_k^{-1}(\theta) S_k^{-1} C_k^\top C_k \tilde{x}^k \\ \hat{y}_k &= C_k \hat{x}^k\end{aligned} \tag{5}$$

where $\hat{x}^k = (\hat{x}^k_1, \cdots, \hat{x}^k_{\lambda_k})^\top$, $\tilde{x}^k = x^k - \hat{x}^k$, $\theta > 0$,

$$\delta_k = \begin{cases} 2^{p-k}\left(\Pi_{i=k+1}^p (\lambda_i - \frac{3}{2})\right), & \text{if } 1 \le k \le p-1 \\ 1, & \text{if } k = p \end{cases}$$

$$\begin{aligned}\Delta_k(\theta) &= \text{diag}\{1, \frac{1}{\theta^{\delta_k}}, \dots, \frac{1}{\theta^{\delta_k(\lambda_k - 1)}}\} \\ \hat{\varphi}^k &= (\hat{\varphi}^k_1, \dots, \hat{\varphi}^k_{\lambda_k})^\top \\ \hat{\varphi}^k_i &= \varphi^k_i(\hat{x}^1, \dots, \hat{x}^{k-1}, \hat{x}^k_1, \dots, \hat{x}^k_i, \hat{x}^{k+1}_1, \dots, \hat{x}^p_1, u)\end{aligned}$$

and S_k is solved from

$$S_k + A_k^\top S_k + S_k A_k = C_k^\top C_k. \tag{6}$$

It has been shown in [15] that the solution to (6) is symmetric positive definite and satisfies $S_k^{-1} C_k^\top = (C^1_{\lambda_k}, \dots, C^{\lambda_k}_{\lambda_k})^\top$ with $C^i_{\lambda_k} = \lambda_k!/(i!(\lambda_k - i)!)$ for $1 \le i \le \lambda_k$.

Given the observer (5), $\hat{\zeta}$ can be constructed by

$$\begin{aligned}\dot{\hat{\zeta}} &= f(\hat{\zeta}) + g(\hat{\zeta}, u) + \frac{\partial \zeta}{\partial x} \Theta \Delta^{-1}(\theta) S^{-1} C^\top (y - \hat{y}) \\ \hat{y} &= h(\hat{\zeta}),\end{aligned} \tag{7}$$

where $\Theta = \text{diag}\{\theta^{\delta_1}, \cdots, \theta^{\delta_p}\}, \Delta^{-1} = \text{diag}\{\Delta_1^{-1}(\theta), \cdots, \Delta_p^{-1}(\theta)\}, S^{-1} = \text{diag}\{S_1^{-1}, \dots, S_p^{-1}\}$. Notice that (7) includes the term $\frac{\partial \zeta}{\partial x}$, which assumes the closed form formula of the inverse transformation $\zeta = \phi^{-1}(x)$.

C. Design Procedure for Case 2: $\zeta = \phi^{-1}(x)$ Unsolvable

Without the closed form expression of $\zeta = \phi^{-1}(x)$, one cannot obtain the system representation in (3). Without knowing the expression of $\varphi(x, u)$, observer (5) can be neither designed nor implemented. This section shows that one can still perform observer design in the non-triangular observable coordinates.

1) Observer design in x-coordinates: The design of observer (5) necessitates the expression of $\varphi(x,u)$ in order to estimate the Lipschitz constant of $\varphi(x,u)$ in x. Next, we show how the Lipschitz constant of $\varphi(x,u)$ in x can be estimated on the basis of $\phi(\zeta)$. Assume that $\varphi(x,u)$ is globally Lipschitz with respect to x uniformly in u, i.e.,

Assumption 3.3: Given system (3), $\forall x_1, x_2 \in \mathbb{R}^n, \exists L_x > 0$

$$|\varphi(x_1,u) - \varphi(x_2,u)| \le L_x |x_1 - x_2|. \tag{8}$$

Note that L_x is unknown and to be estimated. From (8) and considering that $\varphi(x,u)$ is smooth about its arguments, we have for all $u \in \mathbb{R}^m$

$$\begin{aligned}|\varphi(x_1,u) - \varphi(x_2,u)| &\le |\frac{\partial \varphi(x,u)}{\partial x}|_\infty \times |x_1 - x_2| \\ &= |\frac{\partial \varphi(\phi(\zeta),u)}{\partial \zeta}\frac{\partial \zeta}{\partial x}|_\infty \times |x_1 - x_2| \\ &\le |\frac{\partial \varphi(\phi(\zeta),u)}{\partial \zeta}|_\infty \times |\frac{\partial \zeta}{\partial x}|_\infty \times |x_1 - x_2| \\ &\le \kappa_1 |\frac{\partial \zeta}{\partial x}|_\infty \times |x_1 - x_2|, \ \forall x, \zeta \in \mathbb{R}^n,\end{aligned}$$

where $0 < |\frac{\partial \varphi(\phi(\zeta),u)}{\partial \zeta}|_\infty \le \kappa_1$, and

$$\varphi(\phi(\zeta),u) = \frac{\partial \phi(\zeta)}{\partial \zeta}(f(\zeta) + g(\zeta)u) - A\phi(\zeta).$$

Since $\frac{\partial \varphi(\phi(\zeta),u)}{\partial \zeta}$ is known, the upper bound of its infinity norm κ_1 can be established. To derive the upper bound of $|\frac{\partial \zeta}{\partial x}|_\infty$, we take into account the fact that for a non-singular matrix M, its infinity norm (max absolute eigenvalue) equals to the inverse of the min absolute eigenvalue of M^{-1}, i.e.,

$$\max |\text{eig}(M)| = |M|_\infty = \frac{1}{\min |\text{eig}(M^{-1})|}.$$

The above equation produces an upper bound of $|\frac{\partial \zeta}{\partial x}|_\infty$ as $\kappa_2 = 1/\min|\text{eig}(\frac{\partial x}{\partial \zeta})|$. We therefore establish $\kappa_1\kappa_2$ as the upper bound of the Lipschitz constant L_x.

2) Constructing estimates of ζ: With $\varphi(x,u)$ unknown, observer (5) cannot be realized. However, φ, if represented as a function of $(\phi(\zeta),u)$, is implementable. Consequently, the following implementable x-observer can be reached

$$\begin{aligned}\dot{\hat{x}}^k &= A_k \hat{x}^k + \varphi^k(\phi(\hat{\zeta}),u) + \theta^{\delta_k}\Delta_k^{-1}(\theta)S_k^{-1}C_k^\top C_k \tilde{x}^k \\ \hat{y}_k &= C_k \hat{x}^k,\end{aligned} \tag{9}$$

where $\varphi^k(\phi(\hat{\zeta}),u)$ are the rows corresponding to the kth subsystem in $\varphi(\phi(\hat{\zeta}),u)$ given by

$$\varphi(\phi(\hat{\zeta}),u) = \frac{\partial \phi(\hat{\zeta})}{\partial \hat{\zeta}}(f(\hat{\zeta}) + g(\hat{\zeta})u) - A\phi(\hat{\zeta})$$

and $\hat{\zeta}$ is numerically solved from the following n nonlinear algebraic equations

$$\hat{x} = \phi(\hat{\zeta}). \tag{10}$$

As a result, observer (9) is implemented as (10) and

$$\begin{aligned}\dot{\hat{x}} &= \frac{\partial \phi(\hat{\zeta},u)}{\partial \hat{\zeta}}(f(\hat{\zeta}) + g(\hat{\zeta})u) + \Theta\Delta^{-1}(\theta)S^{-1}C^\top C\tilde{x} \\ \hat{y} &= C\hat{x}.\end{aligned} \tag{11}$$

Remark 3.4: Solving (10) may generally resort to iterative algorithms for numerical solutions. If the state transformation $\phi(\zeta)$ is a global diffeomorphism, $\hat{\zeta}$ can be uniquely solved from (10). Otherwise, $\phi(\zeta)$ is non-convex, and that iterative algorithms may converge to an incorrect estimate $\hat{\zeta}$.

Alternatively, considering the state transformation $\phi(\zeta)$ is a local diffeomorphism, and thus its Jacobian $\frac{\partial x}{\partial \zeta}$ is non-singular. One can therefore implement the observer (7) as follows

$$\begin{aligned}\dot{\hat{\zeta}} &= f(\hat{\zeta}) + g(\hat{\zeta},u) \\ &\quad + \left(\frac{\partial x}{\partial \zeta}\right)^{-1}\Theta\Delta^{-1}(\theta)S^{-1}C^\top(y - \hat{y}) \\ \hat{y} &= h(\hat{\zeta}).\end{aligned} \tag{12}$$

Note that (12) is different from (7) where the Jacobian of the inverse state transformation, $\frac{\partial \zeta}{\partial x}$, is used.

D. Application to Speed-sensorless Estimation

We give a concise representation of system (1) as follows

$$\dot{\zeta} = f(\zeta) + g^1 u_{ds} + g^2 u_{qs},$$

where $\zeta = (i_{ds}, i_{qs}, \Phi_{dr}, \Phi_{qr}, \omega)^\top$, $g^1 = (1/\sigma, 0, 0, 0, 0)^\top$, $g^2 = (0, 1/\sigma, 0, 0, 0)^\top$, and f is appropriately defined. Then system (1) is verified to be transformable to the non-triangular observable form (3).

1) Verifying that system (1) *admits the form* (3)*:* We show that system (1) is transformable to the non-triangular observable form by the following change of state coordinates, for the kth subsystem

$$x^k = \phi^k(\zeta) = \begin{bmatrix} h_k(\zeta) \\ \vdots \\ L_f^{\lambda_k - 1}h_k(\zeta)\end{bmatrix}, \tag{13}$$

where λ_k is observability indices [22]. Observability assumption ensures that $x = \phi(\zeta) = ((\phi^1(\zeta))^\top, \ldots, (\phi^p(\zeta))^\top)^\top$ defines new coordinates, i.e., $\phi(\zeta)$ is a local diffeomorphism.

For system (1) with outputs $h_1 = i_{ds}$ and $h_2 = i_{qs}$, observability indices can be taken as $(3,2)$ and $(2,3)$. For illustrative purpose, we take $(\lambda_1, \lambda_2) = (3,2)$ and verify that the change of state coordinates, given by

$$x = (h_1, L_f h_1, L_f^2 h_1, h_2, L_f h_2)^\top, \tag{14}$$

transforms (1) into the non-triangular observable form (3). Given (14), the system in x-coordinates is written as

$$\begin{aligned}\dot{x} &= Ax + \underline{\varphi}(x,u) \\ y &= Cx,\end{aligned}$$

where $A = \text{diag}\{A_1, A_2\}$ with $A_1 \in R^{3\times 3}$ and $A_2 \in \mathbb{R}^{2\times 2}$, $C = \text{diag}\{C_1, C_2\}$ with $C_1 \in R^3$ and $C_2 \in \mathbb{R}^2$, and

$$\begin{aligned}\underline{\varphi} &= \left[(\underline{\varphi}^1)^\top \quad (\underline{\varphi}^2)^\top\right]^\top \\ \underline{\varphi}^1 &= \left\{L_{g^1}h_1(\phi^{-1}(x))u_{ds} + L_{g^2}h_1(\phi^{-1}(x))u_{qs}\right\}\frac{\partial}{\partial x_1^1} \\ &\quad + \left\{L_{g^1}L_f h_1(\phi^{-1}(x))u_{ds} + L_{g^2}L_f h_1(\phi^{-1}(x))u_{qs}\right\}\frac{\partial}{\partial x_2^1}\end{aligned}$$

$$
\begin{aligned}
&+\left\{L_f^3 h_1(\phi^{-1}(x)) + L_{g^1} L_f^2 h_1(\phi^{-1}(x)) u_{ds}\right. \\
&\left. + L_{g^2} L_f^2 h_1(\phi^{-1}(x)) u_{qs}\right\} \frac{\partial}{\partial x_3^1} \\
\underline{\varphi}^2 &= \left\{L_{g^1} h_2(\phi^{-1}(x)) u_{ds} + L_{g^2} h_2(\phi^{-1}(x)) u_{qs}\right\} \frac{\partial}{\partial x_1^2} \\
&+\left\{L_f^2 h_2(\phi^{-1}(x)) + L_{g^1} L_f h_2(\phi^{-1}(x)) u_{ds}\right. \\
&\left. + L_{g^2} L_f h_2(\phi^{-1}(x)) u_{qs}\right\} \frac{\partial}{\partial x_2^2}.
\end{aligned}
$$

The rest is to verify that $\underline{\varphi}$ satisfies the triangular condition (4), which can be readily performed, and thus omitted.

Remark 3.5: It is worth noting that the non-triangular observable form is not unique. That is, when transforming the original system (2), one has multiple design options: observability indices as well as the ordering of subsystems.

2) Observer design in x-coordinates: Given the observer (5) for the kth subsystem, an observer can be readily designed for each subsystem. For the induction motor case, we take $\lambda_1 = 3, \lambda_2 = 2, p = 2$, and have design parameters

$$
\begin{aligned}
\theta > 0, \quad \delta_1 = 1, \quad \delta_2 = 1 \\
\Delta_1(\theta) = \mathrm{diag}\{1, \frac{1}{\theta}, \frac{1}{\theta^2}\}, \quad \Delta_1(\theta) = \mathrm{diag}\{1, \frac{1}{\theta}\} \\
S_1^{-1} C_1^\top = (3, 3, 1)^\top, \quad S_2^{-1} C_2^\top = (2, 1)^\top.
\end{aligned}
$$

Substituting the aforementioned design parameters into the kth subsystem, one can obtain observer in x-coordinates as follows

$$
\begin{aligned}
\dot{\hat{x}}^1 &= A_1 \hat{x}^1 + \underline{\hat{\varphi}}^1 + G_1 C_1 \tilde{x}^1 \\
\dot{\hat{x}}^2 &= A_2 \hat{x}^2 + \underline{\hat{\varphi}}^2 + G_2 C_2 \tilde{x}^2 \\
\hat{y}_1 &= C_1 \hat{x}^1 \\
\hat{y}_2 &= C_2 \hat{x}^2,
\end{aligned}
\tag{15}
$$

where $G_1 = \theta^{\delta_1} \Delta_1^{-1}(\theta) S_1^{-1} C_1^\top = \begin{bmatrix} 3\theta & 3\theta^2 & \theta^3 \end{bmatrix}^\top, G_2 = \theta^{\delta_2} \Delta_2^{-1}(\theta) S_2^{-1} C_2^\top = \begin{bmatrix} 2\theta & \theta^2 \end{bmatrix}^\top$.

3) Constructing estimates of ζ: Two approaches can be employed to estimate ζ on the basis of (15). In this section and the following experiments, the estimated state $\hat{\zeta}$ is constructed by implementing the observer in ζ-coordinates, i.e., (12).

E. Stability Analysis

Due to space limitation, we cite main results in [17] for completeness and avoid too much discussions in this paper. Interested readers are referred to this paper's journal version.

Theorem 3.6: [17, Thm. 3.1] Given Assumption 3.3, $\forall M > 0; \exists \theta_0 > 0; \forall \theta \geq \theta_0; \exists \lambda_\theta > 0, \mu_\theta > 0$ such that for $1 \leq k \leq p$

$$
|x(t) - \hat{x}(t)| \leq \lambda_\theta e^{-\mu_\theta t} |x(0) - \hat{x}(0)|
$$

for every admissible control u with $|u|_\infty \leq M$. Moreover, λ_θ is a polynomial in θ and $\lim_{\theta \to \infty} \mu_\theta = +\infty$.

Remark 3.7: Provided that $\phi(\zeta)$ is a local diffeomorphism over an open domain $\mathcal{B}_x$ containing a compact domain $\mathcal{D}$ and $\forall x \in \mathcal{D}$, so does its inverse. The convergence of the zero solution for $\tilde{x}$ also implies the convergence of $\tilde{\zeta}$ because

$$
\begin{aligned}
|\zeta - \hat{\zeta}| &= |\phi^{-1}(x) - \phi^{-1}(\hat{x})| \\
&\leq |\frac{\partial \phi^{-1}(\epsilon)}{\partial \epsilon}|_\infty \lambda_\theta e^{-\mu_\theta t} |x(0) - \hat{x}(0)|,
\end{aligned}
$$

where $|\frac{\partial \phi^{-1}(\epsilon)}{\partial \epsilon}|_\infty$ is computed over all $\epsilon \in \mathcal{B}_x$.

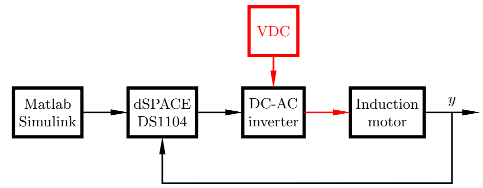

Fig. 1. The testbed architecture.

IV. Experimental Validation

A. The Testbed

The testbed comprises Matlab/Simulink®, dSPACE® ACE Kit DS1104, a DC-AC inverter, and a Marathon®three-phase AC induction motor with no load mounted. The testbed is illustrated by Fig. 2 where the black solid and the red dash represent signals and power flows, respectively. Control algorithm is compiled by Matlab/Simulink®, and downloaded to dSPACE DS1104 for realtime operation. The control algorithm determines desired three-phase voltages, and duty cycles of the six PWM channels; the PWM signals open/close IGBTs of the DC-AC inverter which drive the induction motor.

The dSPACE executes data acquisition and realtime control tasks. Data acquisition task collects the motor position x, and three-phase stator currents i_a, i_b, i_c. The DC-AC inverter is controlled by dSPACE's digital I/O port. During experiments, the dSPACE operates at a sampling frequency of 4kHz, and the PWM frequency is also 4kHz. The encoder has a resolution of 2048 pulses per revolution. The Marathon® motor has parameter values: $R_s = 11.05\Omega, R_r = 6.11\Omega, L_s = L_r = 0.3165H, L_m = 0.2939H, J = 1.2e - 3kgm^2$.

B. The Tracking Controller & State Estimator

The tracking controller implements an Indirect Field Oriented Control (IFOC) given by Fig. 2. Four Proportional and Integral (PI) controllers are used to regulate speed, rotor flux amplitude, and stator currents in d- and q-axis, respectively. With notation defined in Fig. 2, the tracking controller implements the following control law

$$
\begin{aligned}
i_{ds}^* &= K_\Phi^P e_\Phi + K_\Phi^I \int_0^t e_\Phi \mathrm{d}t \\
i_{qs}^* &= K_\omega^P e_\omega + K_\omega^I \int_0^t e_\omega \mathrm{d}t \\
u_{ds}^* &= K_{ids}^P e_{ids} + K_{ids}^I \int_0^t e_{ids} \mathrm{d}t + u_{dsff} \\
u_{qs}^* &= K_{iqs}^P e_{iqs} + K_{iqs}^I \int_0^t e_{iqs} \mathrm{d}t + u_{qsff},
\end{aligned}
\tag{16}
$$

where $u_{dsff} = -\sigma \omega_1 i_{qs}$ and $u_{qsff} = \sigma(\omega_1 i_{ds} + \beta \hat{\omega} \hat{\Phi}_{dr})$. All constants in (16) are obtained by trial and error to achieve satisfactory speed tracking performance. The state estimator consists of an open-loop flux observer to estimate rotor flux amplitude, and a low pass filter to remove the encoder noise. The Clarke/Park transformation and its inverse use the field angle $\hat{\theta}$ computed according to the following formula

$$\dot{\hat{\theta}} = \hat{\omega} + \frac{\alpha L_m i_{qs}^*}{\Phi^*}, \quad \hat{\theta}(0) = 0.$$

C. Experimental Results

Two algorithms are tested in experiments: baseline and the proposed algorithms. The algorithm in [29] is chosen as baseline, where the proportion and integration gains in the speed adaptation law are tuned by trial and error to balance two objectives: the harmonics reduction during steady state and the fast estimation during transient. The proposed algorithm has only one tuning parameter which is taken as $\theta = 20$. Due to the fact that the coordinates (13) is locally defined and not uniformly in u, the inverse jacobian matrix in (12) might be singular or ill-conditioned. During experiments, we approximate the inverse jacobian matrix to avoid non-singularity, which consequently incurs non-zero steady state of the speed estimation error. Readers are referred to the journal version for details on approximation and compensation of non-zero steady state error.

To make fair comparison, the tracking controller uses the measured speed as feedback signal for speed control, i.e., both the baseline and proposed state estimation algorithms run in open-loop. With a focus on the bandwidth of speed estimation, we conduct tests where the reference speed includes step changes, and examine how fast two estimation algorithms converge.

Figs. 3, 5 show trajectories of reference speed ω^*, measured speed ω, estimated speed $\hat{\omega}$, where the solid blue–the reference speed; the solid black–measured speed; the solid green–estimated speed from baseline approach; the solid red–estimated speed from the proposed algorithm; and the dash black–speed tracking error. Figs. 4, 6 show speed estimation error trajectories, where the solid green–estimated error from baseline approach; the solid red–estimated error from the proposed algorithm; and the dash red–zoomed in estimated error from the proposed algorithm. In Fig. 3, the reference speed jumps from $30rad/sec$ to $40rad/sec$ at around $t = 1.27sec$, and from $40rad/sec$ to $30rad/sec$ at around $t = 2.9sec$. One can see that the estimated speed of the proposed algorithm converges to the neighborhood of the measured speed much faster that the baseline does. Fig. 4 shows the speed estimation error trajectories. The upper plot of Fig. 4 shows that the proposed algorithm can effectively reject variations of the speed reference, and the resultant speed estimation error is consistently less than $2rad/sec$. From the zoomed in plot (dash red line) in Fig. 4, one can see that the proposed algorithm has a transient less than $0.02sec$. Several test cases are conducted in a similar manner as above, and the results are shown in Figs. 5-6. Clearly, conclusions from these three cases coincide with that drawn from the first case.

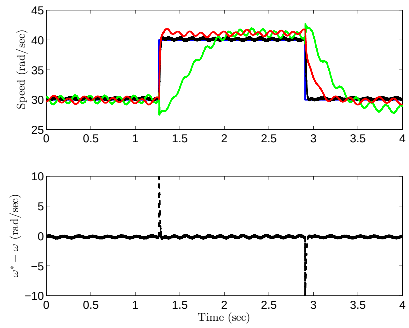

Fig. 3. Speed and tracking error when the reference speed jumps between $30rad/sec$ to $40rad/sec$.

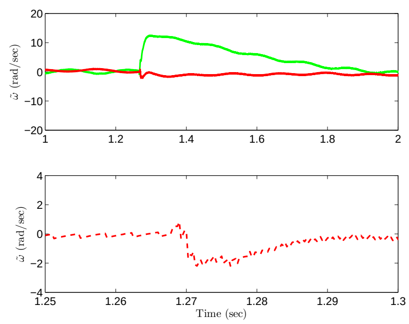

Fig. 4. Speed estimation errors when the reference speed jumps between $30rad/sec$ to $40rad/sec$

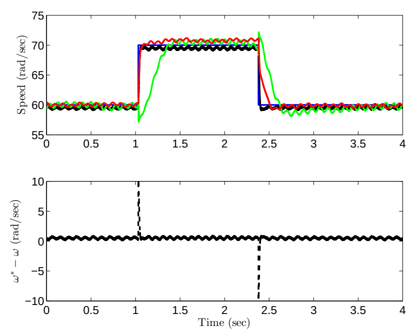

Fig. 5. Speed and tracking error when the reference speed jumps between $60rad/sec$ to $70rad/sec$

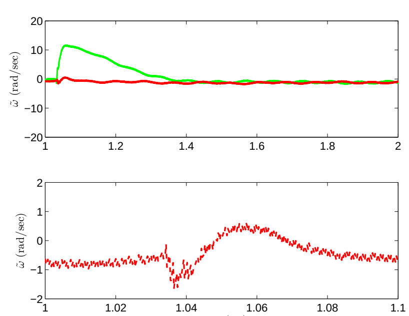

Fig. 6. Speed estimation errors when the reference speed jumps between $60rad/sec$ to $70rad/sec$

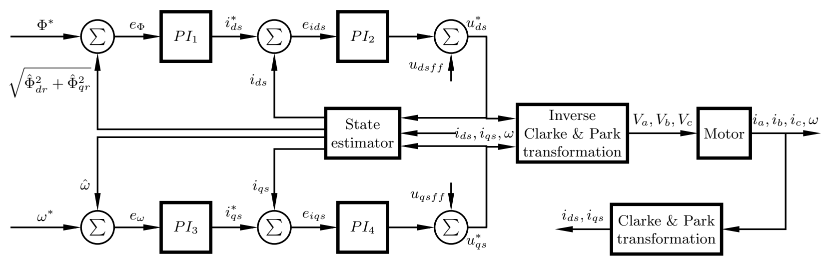

Fig. 2. The IFOC block diagram.

V. Conclusion and Future Work

This paper proposed and verified a new estimation algorithm for speed-sensorless induction motor drives. The proposed algorithm is based on first transforming the induction motor model into a non-triangular observable form by a change of state coordinates, and then performed a high gain observer design in the new coordinates. Applying the transformation-based observer design results in exponentially stable estimation error dynamics. We further provided several observers which can be implemented without solving the inverse state transformation. Experiments demonstrated the effectiveness and advantages of the proposed estimation algorithm: fast speed estimation and ease of tuning. Future work includes experimental validation of speed-sensorless motor drive with the proposed algorithm in the feedback loop.

References

[1] J. Chiasson, "Dynamic feedback linearization of the induction motor," *IEEE Trans. Automat. Control*, vol. 38, no. 10, pp. 1588–1594, 1993.

[2] L. Harnefors, "Globally stable speed-adaptive observers for sensorless induction motor drives," *IEEE Trans. Ind. Electron.*, vol. 54, no. 2, pp. 1243–1245, Apr. 2007.

[3] M. Montanari, S. Peresada, and A. Tilli, "A speed-sensorless indirect field-oriented control for induction motors based on high gain speed estimation," *Automatica*, vol. 42, no. 10, pp. 1637–1650, Oct. 2006.

[4] D. J. Atkinson, P. P. Acarnley, and J. W. Finch, "Observers for induction motor state and parameter estimation," *IEEE Trans. Ind. Appl.*, vol. 27, no. 6, pp. 1119–1127, Nov./Dec. 1991.

[5] C. Schauder, "Adaptive speed identification for vector control of induction motors without rotational transducers," *IEEE Trans. Ind. Appl.*, vol. 28, no. 5, pp. 1054–1061, Sep./Oct. 1992.

[6] H. Kubota, K. Matsuse, and T. Nakano, "DSP-based speed adaptive flux observer of induction motor," *IEEE Trans. Ind. Appl.*, vol. 29, no. 2, pp. 344–348, Mar./Apr. 1993.

[7] Y. R. Kim, S.-K. Sul, and M.-K. Park, "Speed sensorless vector control of induction motor using extended kalman filter," *IEEE Trans. Ind. Appl.*, vol. 30, no. 5, pp. 1225–1233, Sep./Oct. 1994.

[8] K. Ohyama, G. M. Asher, and M. Sumner, "Comparative analysis of experimental performance and stability of sensorless induction motor drives," *IEEE Trans. Ind. Electron.*, vol. 53, no. 1, pp. 178–186, Feb. 2006.

[9] H. K. Khalil, E. G. Strangas, and S. Jurkovic, "Speed observer and reduced nonlinear model for sensorless control of induction motors," *IEEE Trans. Contr. Syst. Technol.*, vol. 17, no. 2, pp. 327–339, 2009.

[10] C. Lascu, I. Boldea, and F. Blaabjerg, "A class of speed-sensorless sliding-mode observers for high-performance induction motor drives," *IEEE Trans. Ind. Electron.*, vol. 56, no. 9, pp. 3394–3403, Sep. 2009.

[11] M. Ghanes and G. Zheng, "On sensorless induction motor drives: sliding-mode observer and output feedback controller," *IEEE Trans. Ind. Electron.*, vol. 56, no. 9, pp. 3404–3413, Sep. 2009.

[12] M. Barut, S. Bogosyan, and M. Gokasan, "Speed-sensorless estimation for induction motors using extended kalman filter," *IEEE Trans. Ind. Electron.*, vol. 54, no. 1, pp. 272–280, Jan. 2007.

[13] M. Hilairet, F. Auger, and E. Berthelot, "Speed and rotor flux estimation of induction machines using a two-stage extended kalman filter," *Automatica*, vol. 45, no. 8, pp. 1819–1827, Aug. 2009.

[14] S. Jafarzadeh, C. Lascu, and M. Sami Fadali, "State estimation of induction motor drives using unscented kalman filter," *IEEE Trans. Ind. Electron.*, vol. 59, no. 11, pp. 4207–4216, Nov. 2012.

[15] J. P. Gauthier, H. Hammouri, and S. Othman, "A simple observer for nonlinear systems–applications to bioreactors," *IEEE Trans. Automat. Control*, vol. 37, no. 6, pp. 875–880, Jun. 1992.

[16] J. A. Moreno and M. Osorio, "A Lyapunov approach to second-order sliding mode controllers and observers," in *Proc. 47th CDC*, Cancun, Mexico, 2008, pp. 2856–2861.

[17] M. Farza, M. M'Saad, M. Triki, and T. Maatoug, "High gain observer for a class of non-triangular systems," *Syst. Control Lett.*, vol. 60, no. 1, pp. 27–35, Jan. 2011.

[18] W. Leonhard, *Control of Electrical Drives*. Springer, 2001.

[19] J. Holtz, "Sensorless control of induction motor drives," *Proceedings of the IEEE*, vol. 90, no. 8, pp. 1359–1394, 2002.

[20] S. Ibarra-Rojas, J. Moreno, and G. Espinosa-Pérez, "Global observability analysis of sensorless induction motors," *Automatica*, vol. 40, no. 6, pp. 1079–1085, Jun. 2004.

[21] A. J. Krener and A. Isidori, "Linearization by output injection and nonlinear observers," *Syst. Control Lett.*, vol. 3, no. 1, pp. 47–52, Jun. 1983.

[22] A. J. Krener and W. Respondek, "Nonlinear observers with linearizable error dynamics," *SIAM J. Control Optim.*, vol. 23, no. 2, pp. 197–216, Mar. 1985.

[23] W. Respondek, A. Pogromsky, and H. Nijmeijer, "Time scaling for observer design with linearizable error dynamics," *Automatica*, vol. 40, no. 2, pp. 277–285, Feb. 2004.

[24] Y. Wang and A. F. Lynch, "Multiple time scalings of a multi-output observer form," *IEEE Trans. Automat. Control*, vol. 55, no. 4, pp. 966–971, Apr. 2010.

[25] J. Rudolph and M. Zeitz, "Block triangular nonlinear observer normal form," *Syst. Control Lett.*, vol. 23, no. 1, pp. 1–8, Jul. 1994.

[26] Y. Wang and A. Lynch, "A block triangular form for nonlinear observer design," *IEEE Trans. Automat. Control*, vol. 51, no. 11, pp. 1803–1808, Nov. 2006.

[27] ——, "A block triangular observer forms for nonlinear observer design," *Int. J. Control*, vol. 81, no. 2, pp. 177–188, 2008.

[28] W. Perruquetti, T. Floquet, and E. Moulav, "Finite-time observers: application to secure communication," *IEEE Trans. Automat. Control*, vol. 53, no. 2, pp. 356–360, Feb. 2008.

[29] H. Kubota and K. Matsuse, "Speed sensorless field-oriented control of induction motor with rotor resistance adaption," *IEEE Trans. Ind. Appl.*, vol. 30, no. 5, pp. 1219–1224, Sep./Oct. 1994.